Proc. Natl. Acad. Sci. USA
Vol. 91, pp. 202–205, January 1994
Biophysics

Enhanced force generation by smooth muscle myosin *in vitro*

PETER VANBUREN†, STEVEN S. WORK‡, AND DAVID M. WARSHAW‡§

Departments of ‡Molecular Physiology and Biophysics and †Cardiology, University of Vermont, Burlington, VT 05405

Communicated by Thomas D. Pollard, September 21, 1993

ABSTRACT **To determine whether the apparent enhanced force-generating capabilities of smooth muscle relative to skeletal muscle are inherent to the myosin cross-bridge, the isometric steady-state force produced by myosin in the *in vitro* motility assay was measured. In this assay, myosin adhered to a glass surface pulls on an actin filament that is attached to an ultracompliant (50–200 nm/pN) glass microneedle. The number of myosin cross-bridge heads able to interact with a length of actin filament was estimated by measuring the density of biochemically active myosin adhered to the surface; with this estimate, the average force per cross-bridge head of smooth and skeletal muscle myosins is 0.6 pN and 0.2 pN, respectively. Surprisingly, smooth muscle myosin generates approximately three times greater average force per cross-bridge head than does skeletal muscle myosin.**

All muscles are believed to generate force through the cyclic interaction of two contractile proteins, myosin and actin. The energy that drives this process is derived from the hydrolysis of ATP by the myosin cross-bridge. Smooth muscle, found in virtually all hollow organs of the body, is unique in its ability to generate as much force per cross-sectional area as skeletal muscle with only one-fifth the myosin content (1). Although this apparent difference could possibly be explained at the tissue or cellular level, when these data are interpreted at the molecular level, smooth muscle cross-bridges may generate greater average force than skeletal muscle cross-bridges. To test this hypothesis, we used an *in vitro* motility assay.

The *in vitro* motility assay has proven a useful tool in studying the molecular mechanism by which myosin generates force and motion as it interacts with actin (2–4). In this assay, fluorescently labeled actin filaments are observed sliding over a myosin-coated surface. Although the velocity of freely moving actin filaments can be readily determined, the measurement of force is far more difficult. In 1988, Kishino and Yanagida (5) described a novel technique for measuring force in this assay. We have adopted this technique (Fig. 1) to compare the force generated by smooth and skeletal muscle myosin.

MATERIALS AND METHODS

All contractile proteins were prepared as described (4). Either turkey gizzard thiophosphorylated smooth muscle or chicken pectoralis skeletal muscle myosin monomers (250 μg/ml) in a myosin buffer (300 mM KCl/5 mM $MgCl_2$/25 mM imidazole/1 mM EGTA/10 mM dithiothreitol, pH 7.4) were incubated on a nitrocellulose-coated glass coverslip for 2 min and then washed with bovine serum albumin at 0.5 mg/ml in myosin buffer. Next, a 0.1-ml-solution bead of low-ionic-strength assay buffer containing fluorescent, tetramethylrhodamine B isothiocyanate-labeled actin filaments (≈45 ng/ml) was placed on top of the myosin surface [assay buffer: 25 mM KCl/5 mM $MgCl_2$/25 mM imidazole/1 mM EGTA/2 mM ATP/10 mM dithiothreitol/0.375% methylcellulose, pH 7.4, with an enzymatic oxygen scavenger system (glucose oxidase at 0.1 mg/ml, catalase at 0.018 mg/ml, and glucose at 2.3 mg/ml)].

Actin filaments (10–30 μm in length), suspended in solution and freely moving on the myosin surface, were observed through an epifluorescence inverted microscope system (6) at ×1000 (Zeiss; ×100 Neofluar, numerical aperature = 1.3). The microneedle, to which an actin filament was attached, was fixed to a three-dimensional micromanipulator (Narashige, Tokyo; model MW-3). The microneedle tip was coated with *N*-ethylmaleimide-treated skeletal muscle myosin (1 mg/ml) by placing the tip for 1 min in a 10-μl solution bead on a siliconized coverslip adjacent to the myosin-coated surface. *N*-Ethylmaleimide myosin is a non-ATP-hydrolyzing, strong-binding myosin analogue that was used to attach the actin filament to the microneedle. The *N*-ethylmaleimide myosin-coated microneedle was then transferred to the actin-containing solution bead. To coax an actin filament over to the microneedle tip, a specially designed pneumatically driven micromanipulated microscope stage was used to move the coverslip and, thus, the actin filament. The microneedle tip was then brought to within 4 μm of the myosin surface, allowing the attached actin filament to engage the myosin surface (Fig. 2). As myosin pulled on the actin filament, the microneedle tip was deflected. This event was recorded on videotape, and the images were digitized at a later time. Microneedle deflection (x) was determined with the use of image-processing software developed in this laboratory (6). Having calibrated the microneedle stiffness (k), we determined the force (i.e., $k * x$) generated over time (Fig. 3). The measured force was corrected for any actin filament angular deviation from the axis perpendicular to the microneedle. In addition, we measured the length of actin in contact with the myosin surface at maximal microneedle deflection. The microscope and all manipulators were mounted on a pneumatic-vibration isolation table. Experiments were conducted at 30°C with the use of an objective heater.

The microneedles were drawn from borosilicate glass capillary tubing (1 mm o.d.) by the technique of Howard and Hudspeth (7) to an initial diameter of 20 μm and then a final diameter of 0.2 μm; the ultracompliant portion was 0.5–1.0 mm in length. The microneedle stiffness was calibrated by electrostatically attaching a polystyrene bead of 40-μm diameter (Polyscience; density 1.005 g/cm³) to the microneedle tip. The vertical deflection of the microneedle ($\delta\times$), resulting from the weight of the bead, and the bead diameter were visualized by video camera through a horizontally placed microscope (Leitz; ×200 magnification). These dimensions were determined from the video image by using a digital image processor (Hamamatsu, Middlesex, NJ; Argus 10). Bead weight (W) was calculated (W = volume * density). Microneedle stiffness ($k = W/\delta X$) ranged typically from 2–20 pN/μm. For each microneedle, this calibration procedure was repeated at least three times with an average 5% error in the stiffness estimate. The accuracy of our stiffness estimates were independently confirmed to within 10% by using cantilever-beam theory to

The publication costs of this article were defrayed in part by page charge payment. This article must therefore be hereby marked "*advertisement*" in accordance with 18 U.S.C. §1734 solely to indicate this fact.

§To whom reprint requests should be addressed.

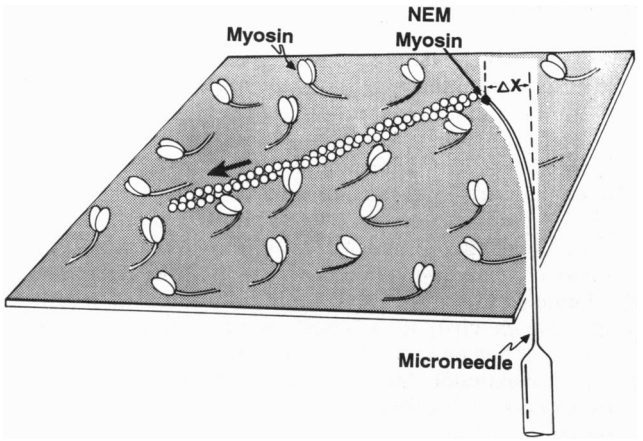

FIG. 1. An actin filament attached to a microneedle interacts with a myosin-coated surface. The microneedle is deflected (ΔX) by the force generated in the actin–myosin interaction. NEM, *N*-ethylmaleimide.

calculate the theoretical microneedle stiffness based on Young's modulus for glass and the microneedle dimensions obtained in a scanning electron microscope.

Myosin head density on the nitrocellulose-coated coverslip was determined by NH_4-EDTA ATPase (8) to estimate the number of biochemically active heads and by an ultrasensitive protein assay to estimate the total amount of myosin bound to the surface (9). ATPase measurements on the coverslip surface were compared with ATPase measurements in the test-tube (in which known amounts of myosin were used) to determine the density of biochemically active heads on the *in vitro* motility assay surface (8). Comparing the results of the ATPase and protein-binding assays, it appears that ≈70% of both smooth and skeletal muscle myosin bound to the surface is biochemically active, as has been reported (10) for skeletal muscle myosin alone. Secondly, both smooth and skeletal muscle myosin surfaces are saturated at myosin loadings >100 μg/ml. We have assumed, as have others (5, 11), that all biochemically active heads are mechanically active.

RESULTS AND DISCUSSION

The time to steady-state force for smooth muscle myosin is an order of magnitude longer than that for skeletal muscle myosin (Fig. 3). This result is not surprising because a similar difference is seen in the velocity of freely moving actin filaments over these two myosin surfaces (4). However, compared with electrically stimulated smooth and skeletal muscle fibers, the rate of force development in this assay is considerably slower. This result is most likely the effect of viscous drag forces, against which the cross-bridges must operate, as the microneedle is deflected through the methylcellulose-containing solution. Therefore, on the basis of simple force–velocity considerations, one might expect the rate at which cross-bridges attain their isometric steady-state force to be greatly diminished in this viscous milieu.

The steady-state forces generated by smooth and skeletal muscle myosins are plotted against the lengths of actin in contact with the surface (Fig. 4). The slopes of these relationships are 34.7 ± 2.3 pN/μm and 12.5 ± 0.8 pN/μm for smooth muscle and skeletal muscle myosins, respectively. If similar densities of mechanically active cross-bridge heads exist on the coverslip, then these results suggest that each smooth muscle cross-bridge head generates three times more average force than a skeletal muscle cross-bridge head. Extrapolating from myosin NH_4-EDTA ATPase measurements on the coverslip (8), the density of biochemically active myosin heads is 2328 ± 572 heads per μm^2 for smooth

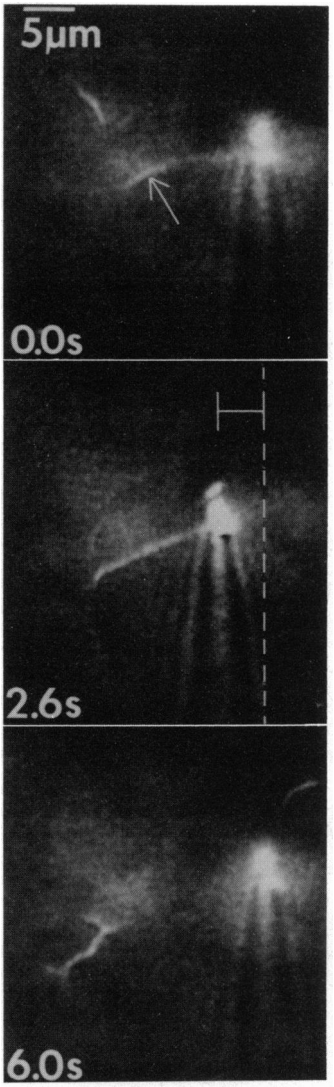

FIG. 2. Three micrographs showing an individual force measurement. (*Top*) At 0.0 s the actin filament, attached to the microneedle, is beginning to engage (indicated by arrow) the skeletal muscle myosin-coated surface. (*Middle*) After 2.6 s, force has reached steady state, and the microneedle is maximally deflected. (*Bottom*) At 6.0 s, the actin filament detaches from the microneedle, allowing the microneedle to return to its original position. The dashed line indicates microneedle position at zero force; the perpendicular solid line marks the extent of needle deflection, which was used to calculate force. The bright microneedle tip is due to numerous fragments of adherent fluorescently labeled actin filaments. Slight bright-field illumination improved visualization of the microneedle outline.

and 2092 ± 349 heads per μm^2 for skeletal muscle myosin. Assuming any smooth or skeletal muscle myosin head within a 10-nm reach (i.e., similar head dimensions for the two myosins) of a 6-nm-diameter actin filament can attach (11), then ≈61 ± 15 smooth muscle and 54 ± 9 skeletal muscle cross-bridge heads per μm of actin filament length can potentially interact with actin and generate force. It is worth noting that our estimate for the number of mechanically active heads agrees with values reported by both the Yanagida (5) and Spudich (11) groups. Their estimates were similarly obtained from ATPase assays under saturated conditions on the myosin surface.

Using these estimates for number of available heads and force per unit length of actin data (Fig. 4), we calculate the average force per cross-bridge head to be 0.6 pN (range,

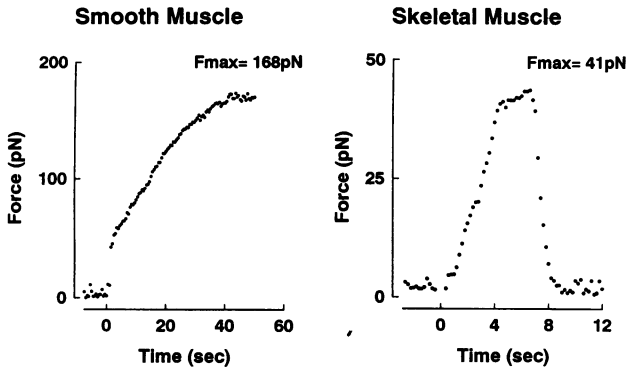

FIG. 3. Force generation over time for two individual force measurements. Microneedle position was determined from digitized video images (6) every 0.5 s and 0.2 s for the smooth muscle and skeletal muscle myosins, respectively. The decline in force seen in the skeletal muscle myosin force measurement is the result of actin filament release from the microneedle (see Fig. 2, for example). Note that the microneedle force returns to baseline. Actin-filament length in contact with the myosin surface was 4.9 and 3.7 μm for smooth muscle and skeletal muscle myosins, respectively. Fmax, maximal force (F) value.

0.4–0.8 pN) for smooth muscle myosin and 0.2 pN (range, 0.2–0.3 pN) for skeletal muscle myosin. The average force per skeletal muscle cross-bridge head that we predict is similar to estimates that Yanagida and coworkers (5, 12, 13) obtained in a comparable assay. We believe that the absolute force values reported here and those of Yanagida and coworkers (5, 12, 13) are probably underestimates, particularly when compared with the 1.4-pN estimate from intact muscle fibers (14). In this assay, myosin is randomly oriented on the coverslip, and its attachment to the surface could affect force generation. Efforts should be made to orient the myosin relative to actin as it exists *in vivo* and to investigate other

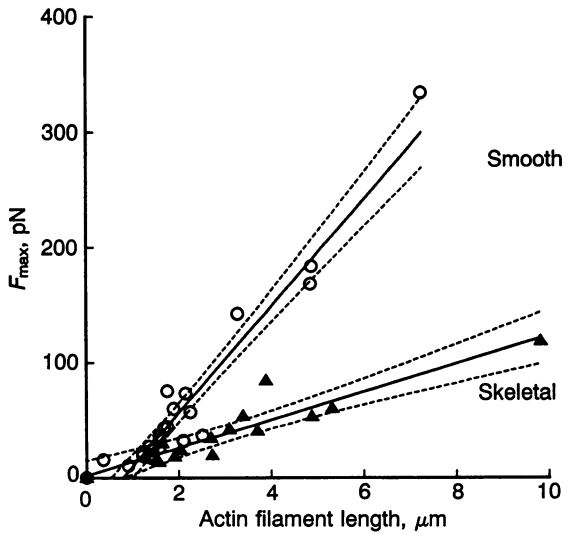

FIG. 4. The steady-state force per actin filament length in contact with the smooth muscle and skeletal muscle myosin surfaces. Each data point results from an individual actin filament measurement. The linear regressions as plotted (solid lines) are 46.2 pN/μm and 12.2 pN/μm for smooth muscle and skeletal muscle myosins, respectively. The 95% confidence limits (dashed lines) were determined by statistical software within the SIGMAPLOT graphics package (Jandel, Corte Madera, CA). When data are constrained through the origin, the regressions for smooth muscle and skeletal muscle myosins differ by a factor of three (see text). This difference is statistically significant ($F = 77$, $p < 0.01$). F_{max}, maximal force (F) value.

methods of attachment that could maximize force transduction.

An interesting dilemma arises when estimates of cross-bridge force from the motility assay at low ionic strength (40 mM) are used to estimate cross-bridge forces *in vivo*. At this low ionic strength, the binding affinities for smooth and skeletal muscle subfragment 1 (S-1) to actin in the presence of nucleotide are approximately equal (15). However, at near physiological ionic strength, the binding of smooth muscle S-1 is only slightly diminished (3-fold), whereas the binding of skeletal muscle S-1 is reduced by as much as 100-fold (15). If S-1 binding to actin in the test-tube is any indication of force production *in vivo*, then based on our cross-bridge force estimates at low ionic strength, one would predict at least two orders of magnitude difference between smooth and skeletal muscle cross-bridge forces *in vivo*, which is not the case. It is possible that the spatial constraints placed on actin and myosin cross-bridges within a muscle fiber increase the probability of cross-bridge attachment and, thus, compensate for the weaker binding affinity of skeletal muscle myosin at physiological ionic strength compared with that of smooth muscle myosin (15).

The force data presented here strongly suggest that, under identical experimental conditions, smooth muscle cross-bridge heads appear to generate three times more average force than skeletal muscle cross-bridge heads. A similar conclusion was drawn from motility studies in which both smooth muscle and skeletal muscle myosins were mixed independently with *N,N'-p*-phenylenedimaleimide skeletal muscle myosin (4). This sulfhydral-modified myosin, which no longer hydrolyzes ATP and binds weakly to actin, serves as an internal load to impede actin filament motion created by the normally cycling smooth and skeletal muscle myosins. In this earlier study, the relative amount of *N,N-p*-phenylenedimaleimide myosin required to halt actin-filament motility was approximately three to four times greater in a mixture with smooth muscle myosin than in a mixture with skeletal muscle myosin. By this indirect approach, we previously predicted a similar enhancement in the force-generating potential of smooth muscle myosin.

Can alterations in the kinetics of the cross-bridge cycle or the manner in which chemical energy is converted to mechanical work explain the greater force production of smooth muscle myosin? A simple two-state cross-bridge model, first proposed by Huxley (16) in 1957, can be used to depict the interaction of myosin with actin. Specifically, the cross-bridge is first detached or weakly attached to actin and then becomes more strongly attached as it undergoes the power stroke to generate its unitary force (F_{uni}). The fraction of the cross-bridge cycle in which myosin is strongly bound to actin and generating force is termed the duty cycle (f). The average cross-bridge force that we measure is the resultant product of the unitary force and duty cycle ($F_{avg} = F_{uni} * f$). Therefore, the greater average force (F_{avg}) per cross-bridge head for smooth muscle myosin could be explained by a greater unitary force, an increased duty cycle, or a combination of the two. In the *in vitro* motility assay, we have shown that duty cycles for both smooth and skeletal muscle myosin do not differ (8). However, these data were obtained from actin filaments moving under zero load. Given the dependence of cross-bridge function on strain (17), extrapolating these data to isometric conditions may not be appropriate. Under isometric conditions, evidence for an increased duty cycle in smooth muscle has been obtained from mechanical measurements of single muscle cells (18, 19). In skeletal muscle, duty-cycle estimates are as high as 75% (20) under isometric conditions. Therefore, both unitary force and duty cycle are probably increased to contribute to the 3-fold higher average force per smooth muscle cross-bridge head. Until the development of techniques that have both temporal

and force resolution to measure unitary cross-bridge events, we can only speculate as to how duty cycle and unitary force differ between smooth muscle and skeletal muscle myosins.

The greater force estimated for smooth muscle myosin does not appear to violate energetic constraints. If efficiency of energy transduction by smooth muscle myosin is 15% (21), then 12×10^{-21} J per ATP would be available for work. Under isometric conditions, the only work performed by the cross-bridge would be to stretch the Hookean elastic element, believed to exist within the cross-bridge itself. Assuming that the average force per head is underestimated by a factor of 4 and the duty cycle is 50%, the unitary force would be 4.8 pN. During the cross-bridge working stroke, the internal elastic component may be stretched by a maximum of 4–6 nm (22, 23). Under these conditions the energy expended would be $\approx 12 \times 10^{-21}$ J per cross-bridge cycle. Even in this worst-case estimate, sufficient energy is available from the hydrolysis of a single ATP molecule to sustain the greater force per smooth muscle myosin head.

Although at the cellular level greater numbers of cross-bridges working in parallel due to longer myosin filaments (24) or a parallel arrangement of contractile units within the cell (25) could contribute to the greater force per myosin content of smooth muscle tissue, we have shown that a significant portion of the enhanced force generation can be traced directly to the cross-bridge. Clues as to how this unique functional difference between smooth muscle myosin and skeletal muscle myosin has evolved may be found in the amino acid heterogeneity that exists between these two myosin species, ultimately affecting the molecular structure and function of myosin.

We thank Toshio Yanagida, Yale Goldman, and Jonathan Howard for assistance in the development and implementation of the force-recording assay; Kathleen Trybus for supplying many of the contractile proteins used and for many enjoyable discussions; University of Vermont Instrumentation and Model Facility for the design of much of the hardware; Janet Vose and Chris Stromski for their technical assistance; John Dodge for the scanning electron micrographs of the microneedle; the members of the Departmental Muscle Club for numerous provocative and helpful discussions; and Hugh Huxley, Ed Taylor, and David Harris for their comments on this manuscript. This work was supported by funds from the National Institutes of Health (HL45161, AR42231 to D.M.W. and HL07647 to P.V.B.). D.M.W. is an Established Investigator of the American Heart Association.

1. Murphy, R. A., Herlihy, J. T. & Megerman, J. (1974) *J. Gen. Physiol.* **64,** 691–705.
2. Kron, S. J. & Spudich, J. A. (1986) *Proc. Natl. Acad. Sci. USA* **83,** 6272–6276.
3. Harada, Y., Noguchi, A., Kishino, A. & Yanagida, T. (1988) *Nature (London)* **326,** 805–808.
4. Warshaw, D. M., Desrosiers, J. M., Work, S. S. & Trybus, K. M. (1990) *J. Cell Biol.* **111,** 453–463.
5. Kishino, A. & Yanagida, T. (1988) *Nature (London)* **334,** 74–76.
6. Work, S. S. & Warshaw, D. M. (1992) *Anal. Biochem.* **202,** 275–285.
7. Howard, J. & Hudspeth, A. J. (1985) *Neuron* **1,** 189–199.
8. Harris, D. E. & Warshaw, D. M. (1993) *J. Biol. Chem.* **268,** 14764–14768.
9. Warshaw, D. M., Desrosiers, J. M., Work, S. S. & Trybus, K. M. (1991) *J. Biol. Chem.* **266,** 24339–24343.
10. Hayashi, H., Takiguchi, K. & Higashi-Fujime, S. (1989) *J. Biochem.* **105,** 875–879.
11. Uyeda, T. Q. P., Kron, S. J. & Spudich, J. A. (1990) *J. Mol. Biol.* **214,** 699–710.
12. Johara, M., Toyoshima, Y. Y., Ishijima, A., Hiroaki, K., Yanagida, T. & Sutoh, K. (1993) *Proc. Natl. Acad. Sci. USA* **90,** 2127–2131.
13. Ishijima, A., Doi, T., Sakurada, K. & Yanagida, T. (1991) *Nature (London)* **352,** 301–306.
14. Lombardi, V., Piazzesi, G. & Linari, M. (1992) *Nature (London)* **355,** 638–641.
15. Greene, L. E., Sellers, J. R., Eisenberg, E. & Adelstein, R. S. (1983) *Biochemistry* **22,** 530–535.
16. Huxley, A. F. (1957) *Prog. Biophys. Biophys. Chem.* **7,** 255–318.
17. Ford, L. E., Huxley, A. F. & Simmons, R. M. (1977) *J. Physiol. (London)* **269,** 441–515.
18. Warshaw, D. M. (1987) *J. Gen. Physiol.* **89,** 771–789.
19. Yamakawa, M., Harris, D. E., Fay, F. S. & Warshaw, D. M. (1990) *J. Gen. Physiol.* **95,** 697–715.
20. Goldman, Y. E. & Simmons, R. M. (1977) *J. Physiol. (London)* **269,** 55P–57P.
21. Butler, T. M. & Siegman, M. J. (1985) *Annu. Rev. Physiol.* **47,** 629–643.
22. Arheden, A. & Hellstrand, P. (1991) *J. Physiol. (London)* **442,** 601–630.
23. Warshaw, D. M., Rees, D. D. & Fay, F. S. (1988) *J. Gen. Physiol.* **91,** 761–779.
24. Ashton, F. T., Somlyo, A. V. & Somlyo, A. P. (1975) *J. Mol. Biol.* **98,** 17–29.
25. Warshaw, D. M., McBride, W. J. & Work, S. S. (1987) *Science* **236,** 1457–1459.